Journal of Petroleum Science and Engineering 124 (2014) 122–131

Contents lists available at ScienceDirect

Journal of Petroleum Science and Engineering

journal homepage: www.elsevier.com/locate/petrol

Enhanced oil recovery from high-temperature, high-salinity naturally fractured carbonate reservoirs by surfactant flood

Jun Lu *, Ali Goudarzi, Peila Chen, Do Hoon Kim, Mojdeh Delshad, Kishore K. Mohanty, Kamy Sepehrnoori, Upali P. Weerasooriya, Gary A. Pope

Department of Petroleum and Geosystems Engineering, The University of Texas at Austin, Austin, TX 78712-0228, USA

ARTICLE INFO

Article history:
Received 23 July 2014
Accepted 17 October 2014
Available online 28 October 2014

Keywords:
chemical EOR
surfactant flooding
naturally fractured carbonate reservoirs

ABSTRACT

Water floods are often very inefficient in naturally fractured carbonate oil reservoirs because many of these reservoirs are mixed-wet or oil-wet as well as extremely heterogeneous. Naturally fractured reservoirs are challenging targets for chemical flooding because they typically have a high permeability contrast between the fractures and the matrix with a low matrix permeability. Some of the world's largest oil reservoirs are fractured carbonates with a high reservoir temperature and a high salinity formation brine. Some of them also have low API gravity oils, which also increases the difficulty of recovering the oil. A surfactant formulation has been developed that shows promising results for such difficult reservoirs. Ultra-low interfacial tension (IFT) and good aqueous stability were achieved with this new carboxylate surfactant in a hard brine at a high reservoir temperature of 100 °C. Both static and dynamic imbibition experiments were conducted using a fractured carbonate core. 65.9% Oil recovery was obtained in fractured coreflood compared to 33.3% oil recovery in static imbibition test. The surfactant retention was low at 0.086 mg/g of rock. The oil recovery is excellent taking into account that the temperature and salinity conditions were harsh, the core was extremely vuggy and fractured, no mobility control was used, and only a small surfactant slug was injected. The coreflood results were interpreted using a mechanistic chemical reservoir simulator. It showed that both the mechanisms of IFT reduction and wettability alteration were important for oil recovery. Neither IFT reduction nor wettability alteration alone recovered oil as high as the combined contributions from both.

1. Introduction

Carbonate reservoirs hold approximately 60% of the world's oil reserves (Akbar et al., 2000). A large number of carbonate reservoirs are naturally fractured and are mixed-wet to oil-wet (Roehl and Choquette, 1985; Chillenger and Yen, 1983). Most of carbonate reservoirs have a high degree of heterogeneity and complex pore structure. Naturally fractured carbonate reservoirs typically have high permeability fractures and a low permeability matrix. This high contrast of permeability between matrix and fractures leads to poor water flood efficiency. The oil recovery from naturally fractured carbonate reservoirs is typically much less than one-third.

Wettability has been long recognized as an important factor strongly affecting oil recovery using EOR methods (Zhou et al., 2000; Morrow and Mason, 2001; Tong et al., 2002; Hirasaki and Zhang, 2004). Water floods are often inefficient because many of these reservoirs are mixed-wet or oil-wet as well as extremely heterogeneous. Changing the wettability of the fractured reservoirs from oil or mixed-wet toward water-wet improves oil recovery efficiency. A lot of research has been conducted on wettability alteration by surfactants (Austad et al., 1998; Zhang et al., 2004; Seethepalli et al., 2004; Xie et al., 2004; Chen and Mohanty, 2013; Sharma and Mohanty, 2013; Sagi et al., 2013; Wang and Mohanty, 2014; Bourbiaux et al., 2014).

Static imbibition experiments have been widely used to evaluate different EOR surfactants. The recovery from fractured carbonate reservoirs is frequently considered to be dominated by gravity and capillary forces. However, the role of viscous forces may also be important and should be investigated (Delshad et al., 2009). The Marangoni effect (Austad and Milter, 1997) and spontaneous emulsification (Zhang et al., 2008) might also promote imbibition in some static imbibition experiments. Goudarzi et al. (2012) have suggested that changing the matrix block size affects the oil recovery from static imbibition experiments.

Imbibition experiments using surfactants that produce low IFT have been conducted by several investigators (Hirasaki and

* Corresponding author.
E-mail address: junlu@utexas.edu (J. Lu).

http://dx.doi.org/10.1016/j.petrol.2014.10.016
0920-4105/

Zhang, 2004; Seethepalli et al., 2004; Adibhatla and Mohanty, 2006; Lu, 2014). Hirasaki and Zhang (2004) suggested the dominant oil recovery mechanism in low IFT imbibition to be buoyancy and wettability alteration. With some anionic surfactants, the IFT can be reduced to ultra-low values where the capillary pressure is reduced to nearly zero. When the capillary pressure is nearly zero, then other forces (gravity and viscous) can cause imbibition observed in many experiments. The simulation results by Abbasi-Asl et al. (2010) showed that transverse pressure gradients between the fractures and matrix can push the surfactant further into the matrix in the dynamic imbibition process.

The goal of this work was to study the use of surfactants to enhance the oil recovery from an oil-wet, high-temperature (100 °C), high-salinity fractured carbonate reservoir. With the improved understanding of the relationship between the surfactant structure and performance (Solairaj et al., 2012; Adkins et al., 2012; Lu et al., 2014a, 2014b, 2014c), we were able to develop a surfactant formulation that shows promising results for this reservoir. The surfactant formulation was tested by conducting both static and dynamic experiments. Numerical simulations were used to help us understand and interpret the experimental results. In the next section, the methods are described followed by our experimental and numerical simulation results.

2. Experimental methods

2.1. Materials

Guerbet alkoxy carboxylates were synthesized from Guerbet alkoxylates in our laboratory (Adkins et al., 2012; Lu et al., 2014a). Internal olefin sulfonates (IOS) were obtained from Stepan Company. Sodium chloride, calcium chloride dihydrate, magnesium chloride hexahydrate, and sodium sulfate were obtained from Fisher Chemical and used as received. The synthetic sea water (SSW) and the synthetic formation brine (SFB) were prepared according to the compositions shown in Table 1. Mixtures of sea water and formation brine were used for phase behavior and coreflood experiments. A dead crude oil was provided by an oil company. A surrogate oil (a mixture of dead crude and a low-EACN hydrocarbon to match the live oil EACN) was used for the experiments at ambient pressure to account for the effect of solution gas on phase behavior (Roshanfekr et al., 2012; Jang et al., 2014). The surrogate oil contained 30 wt% cyclohexane and 70 wt% dead crude oil. The density of the oil is 0.92 g/cm^3 (API=22), and the viscosity of surrogate is 2.1 mPa-s (2.1 cp) at the reservoir temperature, 100 °C. The total acid number of the oil is low, 0.15 mg KOH/g oil, and the oil does not appear to be an active oil based on phase behavior scans using sodium carbonate alkali.

2.2. Phase behavior experiments

Surfactant phase behavior tests were conducted to identify effective surfactant formulations for this specific oil at the reservoir temperature. The procedure can be found in Levitt et al. (2006), Flaaten et al. (2008), Zhao et al. (2008), and Lu et al. (2014a) among other papers. The surfactant mixtures with oil and brine were carefully observed over an extended period of time.

Table 1
Sea Water (SSW) and Formation Brine (SFB) composition.

Brine	Na^+ (ppm)	Ca^{2+} (ppm)	Mg^{2+} (ppm)	SO_4^{2-} (ppm)	Cl^- (ppm)	TDS (ppm)
SSW	12,188	480	1342	3250	21,133	38,393
SFB	41,473	3880	145	500	70,971	116,969

The surfactants that form a low viscosity microemulsion and show ultra-low IFT with both oil and water were selected for further evaluation. The phase volumes can be read and used to calculate IFT with the Huh equation (Huh, 1979). The aqueous surfactant solution was observed for stability and clarity at both room temperature and reservoir temperature to determine if it was stable up to at least optimum salinity.

2.3. Contact angle measurements and static imbibition experiment

The surfactant formulations with low IFT were used for contact angle measurements on a calcite plate and for static imbibition experiments in a reservoir core. Contact angle measurements were conducted on the calcite plate with the selected surfactant formulation. The plates (approximately 3.8 cm × 3.8 cm × 0.5 cm) were polished and cleaned to obtain a fresh and smooth surface that is free of any contamination. The cleaned plates were immersed in the formation brine (no surfactant) for a day, and then aged in crude oil at an elevated temperature (80 °C) and ambient pressure for four weeks. The aged plate was then put in a special 5.1 cm × 5.1 cm optical glass cuvette and surrounded with brine or surfactant solution at 100 °C to monitor the evolution of contact angle with time.

The static imbibition experiment was performed with a reservoir core plug. The reservoir core was prepared by cleaning and saturating with the formation brine. The properties of the core plug are listed in Table 2. Oil was then injected into the core to reach initial oil saturation; then it was aged at the reservoir temperature for about a month. Because of its high heterogeneity, a high initial oil saturation (S_{oi}) could not be achieved. Imbibition cells were constructed in the Custom Lab Glass Services at The University of Texas, Austin. The oil-aged core was placed inside the imbibition cell. Then the imbibition cell was filled with the formation brine or the surfactant solution to its neck. If the surfactant solution imbibed into the core plug then the oil was pushed out of the core and accumulated in the neck of glass cell. The volume of the produced oil was monitored on a daily basis (or as often as appropriate). The static imbibition test was performed at the reservoir temperature of 100 °C.

2.4. Coreflood

A reservoir core of about 27.4 cm (10.8 in.) in length and 10.2 cm (4.0 in.) in diameter was obtained, then dried and weighed. The core was wrapped with a Teflon heat shrink tube and then inserted into a 10.2-cm (4-in.) diameter core holder with a confining pressure of 6.89×10^6 Pa (1000 psi). The core was cleaned by injecting toluene, methanol, and synthetic formation brine. Pressure data were recorded and the brine permeability was measured to be about 5.9×10^{-15} m^2 (6 md), which is close to the average matrix permeability of the reservoir.

The core was then taken out of the core holder and cut into three pieces. Each piece of core plug was 7.6–10.2 cm (3–4 in.) long. Axial fractures were created by the adapted wedge splitting test method (Brühwiler and Wittmann, 1990) to mimic the natural fractures in the reservoir. The three core plugs were then stacked together to make a 27.4 cm (10.8 in.) length composite core. The core was dried and put back into the core holder again. The core was evacuated by a vacuum pump and then saturated with the formation brine to measure the pore volume of about 216 ml by material balance. The core holder was placed in the 100 °C oven with a back pressure of 6.89×10^5 Pa (100 psi), and flooded with the formation brine. The brine permeability of the composite fractured core was 1.9×10^{-12} m^2 (1970 md). Oil was then flooded from the top of the vertical core at a frontal velocity of 2.1×10^{-5} m/s (6 ft/day) until no brine was produced. A second

Table 2
Comparison of static imbibition and fractured coreflood results.

Experiment	Static imbibition	Fractured coreflood
Core name	Reservoir core	Reservoir core
Type	Carbonate	Carbonate
Length (cm)	7.86	27.4
Diameter (cm)	3.78	10.2
Pore volume (ml)	7.25	216.0
Porosity	0.082	0.097
Brine permeability (md/m^2)	$42.9/4.2\times10^{-14}$	$6/5.9\times10^{-15}$ (before fractured) $1970/1.9\times10^{-12}$ (after fractured)
S_{oi}	0.586	0.495
S_{orw}	–	0.412
Oil recovery (%)	33.3	64.9
S_{orc}	0.390	0.140

Table 3
Summary of fractured coreflood experiment.

Temperature (°C)	100
Initial salinity (ppm)	116,969
Surfactant slug	
Surfactant concentration (wt%)	1
Pore volumes (PV) injected	0.25
PV × concentration (%)	25
Viscosity (cp/mPa-s)	0.33/0.33
Salinity (ppm)	57,000
Velocity (ft/day/m/s)	$0.2/7.1\times10^{-7}$
Brine drive	
PV injected	1.46
Viscosity (cp/mPa-s)	0.33/0.33
Salinity (ppm)	10,000
Velocity (ft/day/m/s)	$0.2/7.1\times10^{-7}$
Results	
Recovery (%)	64.9
Final residual oil saturation, S_{orc}	0.140
Surfactant retention (mg/g)	0.086

oil flood was conducted after the core was aged to displace more brine and measure the oil permeability and residual water saturation, and it was then followed by a water flood with the formation brine. The residual oil saturation and water relative permeability were measured.

The chemical flood experiment was designed with a favorable salinity gradient to maximize the robustness of the flood (Pope et al., 1979). The salinities of the surfactant slug and brine drive were determined from phase behavior data. A differential pressure transducer was used to measure the pressure drop across the entire core. Effluent from the core was collected by a fraction collector and sampled in glass test tubes to analyze the oil content, surfactant concentration, and salinity. A comparison of the results of the static imbibition experiment and the fractured coreflood is given in Table 2. The results of the fractured coreflood experiment are summarized in Table 3.

2.5. CT scan

A modified medical CT scanner (HD-350E, Universal Systems) was used to scan the core before and after being fractured. The core was scanned at the energy level of 80 kV from the top to the bottom. Each scan contains 512×512 X-ray attenuation values representing the electron density (and thus mass density) of the material inside each $0.2\times0.2\times10\ mm^3$ voxel. The reservoir core was highly vuggy and heterogeneous by visual observations and CT scan analysis.

3. Numerical simulation methods

3.1. Simulator

UTCHEM is a numerical reservoir simulator that models chemical processes such as surfactant flooding. For modeling wettability alteration, the initial and final wettability conditions are defined by two sets of input parameters. Each set includes relative permeability, capillary pressure and residual saturation-trapping number parameters. The altered relative permeability and capillary pressure values used for the multiphase flow calculations are interpolated between the two sets as follows:

$$k_{r\ell}^{altered}=\omega_1 k_{r\ell}^{final}+(1-\omega_1)k_{r\ell}^{initial} \tag{1}$$

$$P_c^{altered}=\omega_2 P_c^{final}+(1-\omega_2)P_c^{initial} \tag{2}$$

where 'final' and 'initial' are the extreme wetting states and 'altered' is the interpolated state due to the surfactant. The scaling factors ω_1 and ω_2 can be constants or dependent on adsorbed surfactant concentration.

Relative permeability and capillary pressure corresponding to initial and final wetting states are calculated in every gridblock based on the Corey model as following:

$$k_{r\ell}=k_{r\ell}^{o}S_{n\ell}^{n_\ell}, \tag{3}$$

where ℓ refers to water, oil or microemulsion phase, $k_{r\ell}^{o}$ is the endpoint relative permeability for phase ℓ and n_ℓ is the Corey exponent of phase ℓ and $S_{n\ell}$ is the normalized saturation of phase ℓ as computed by

$$S_{n\ell}=\frac{S_\ell-S_{\ell r}}{1-\sum_{\ell=1}^{n_p}S_{\ell r}},\quad \ell=\text{water, oil or microemulsion phase} \tag{4}$$

where S_ℓ is the saturation of phase ℓ and $S_{\ell r}$ is the residual saturation of phase ℓ.

The capillary pressure in UTCHEM is modeled as

$$P_c=C_{pc}\frac{\sigma_{om}}{\sigma_{ow}}(1-S_\ell)^{E_{pc}}, \tag{5}$$

where C_{pc} and E_{pc} are endpoint and exponent for capillary pressure, respectively, and IFT for oil/ME and oil/water phases are represented by σ_{om} and σ_{ow}, respectively. In this work, capillary pressure was neglected.

3.2. Modeling imbibition experiment

The imbibition experiment was simulated using a $7\times7\times7$ Cartesian grid. The numerical model includes both the core and the surrounding space filled with surfactant. The first and last gridblock in each direction is used for the surrounding space. The simulations are based on both IFT reduction and wettability alteration using the constant ω_1 factor as described by Goudarzi et al. (2012). The surfactant causes a more favorable oil relative permeability by wettability alteration from mixed-wet to water-wet and also lowers the residual oil saturation by decreasing the interfacial tension.

3.3. Modeling coreflood experiment

Two different approaches can be adopted for modeling coreflood experiments in highly vuggy and fractured cores: (a) heterogeneous permeability distribution, (b) explicit fracture model. If the streamlines pass through both vugs and fractures, then random permeability distribution approach can be more accurate. However, if the fractures are all connected and flow happens mainly through the fracture channels, then using explicit fracture modeling is more accurate. Because of the contribution of

both vugs and fractures in the mentioned coreflood experiment, a random heterogeneous permeability distribution was used to model the extremely heterogeneous fractured and vuggy core. A Cartesian $5 \times 5 \times 10$ grid was used as shown in Fig. 1. The average brine permeability was 1.9×10^{-12} m^2 (1970 md). A Dykstra–Parsons coefficient of 0.9 was required to match the experimental results. This very high value is consistent with the observed high degree of heterogeneity.

4. Results and discussion

4.1. Phase behavior

Adkins et al. (2012) developed a new class of large hydrophobe alkoxy carboxylate surfactants. One of these surfactants was applied in the present study. These novel Guerbet alkoxy carboxylate (GAC) surfactants are produced by the carboxymethylation (carboxylation) of large Guerbet alkoxylates. Guerbet alkoxylates are made by adding alkoxy groups such as propylene oxide (PO) and ethylene oxide (EO) as extenders to the large hydrophobe Guerbet alcohols which are produced from smaller linear alcohols using the Guerbet reaction. The carboxylation reaction can be conducted by using the terminal hydroxide group of an alkoxylate and sodium chloroacetate with sodium hydroxide, or alternatively using chloroacetic acid in the presence of two mole equivalents of sodium hydroxide as shown in Fig. 2, where *R* represents the carbon chain.

Adkins et al. (2012) and Lu et al. (2014a) showed that the GAC surfactants have many advantages over other types of surfactants (Iglauer et al., 2009, 2010) under a very wide range of conditions. The surfactant formulation developed in this study was a mixture of 0.5 wt% C_{28}-25PO-25EO-carboxylate and 0.5 wt% C_{15-18}-IOS. No co-solvent and alkali were needed for this formulation. Fig. 3 shows the oil and water solubilization ratios for this surfactant formulation as a function of salinity. The salinities were achieved by mixing sea water and formation brine in different proportions, which mimic mixing during transport through the reservoir. Winsor type I, III and II phase behavior was observed as the salinity was increased. This formulation equilibrates fast and shows a high optimum solubilization ratio of about 16 at the optimum salinity of about 57,000 ppm as shown in Fig. 3. The solubilization ratio of 16 corresponds to an ultra-low IFT of about 1.2×10^{-3} mN/m using the Huh equation (Huh, 1979). This formulation has excellent tolerance of divalent cations such as calcium and magnesium. The aqueous solutions were clear and stable up to 58,000 ppm TDS for more than 32 days at the reservoir temperature of 100 °C. This surfactant formulation was used in both static imbibition and fractured coreflood experiments.

4.2. Contact angle and static imbibition

The contact angle measurements were conducted on a calcite plate. Fig. 4(a) shows the calcite plate immersed in the formation brine at 100 °C after aging. The contact angle is close to 180° representing oil-wetness. The calcite plate was then placed in surfactant solution at 100 °C in Fig. 4(b). The surfactant solution solubilized almost all of the oil leaving it clean and mostly if not entirely water wet.

The objective of the static imbibition test was to evaluate and select a suitable surfactant for additional tests including the first ever dynamic coreflood experiment using a fractured reservoir core under these very difficult reservoir conditions. The static imbibition experiment was done using a reservoir core plug 3.78 cm (1.5 in.) in diameter by 7.86 cm (3.09 in.) long. The core was saturated with the formation brine and then flooded with crude oil to reach residual water saturation. The core was then immersed in the oil and aged at the reservoir temperature for about a month. After the aging process, the reservoir core was immersed in the formation brine to observe its wettability. No oil

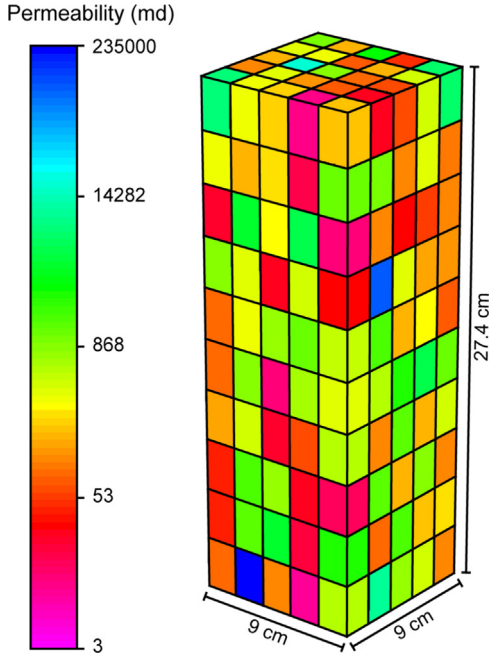

Fig. 1. Permeability distribution (in Darcy units) used for modeling the fractured coreflood.

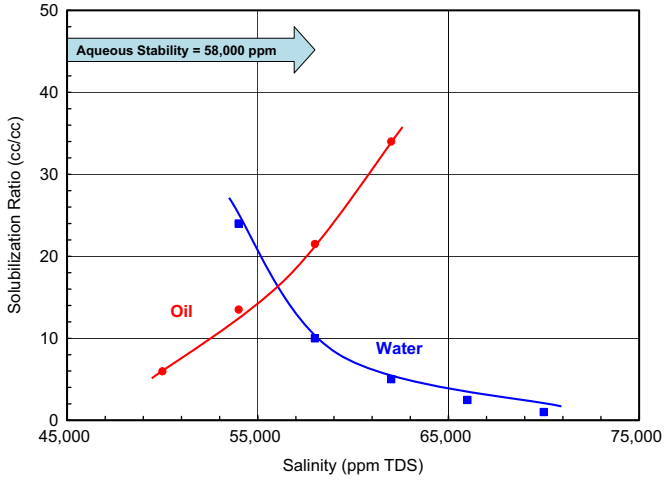

Fig. 3. Phase behavior of 0.5 wt% C_{28}-25PO-25EO-carboxylate and 0.5 wt% C_{15-18}-IOS surfactant mixture at 100 °C with 50 vol% oil after 32 days.

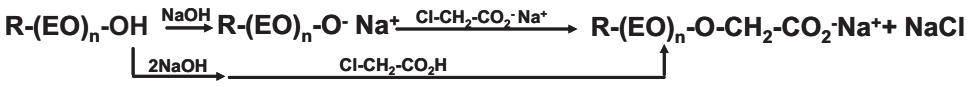

Fig. 2. The reaction to form the alkoxy carboxylate.

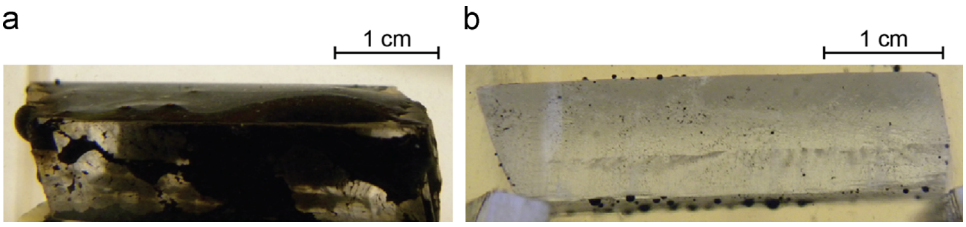

Fig. 4. Oil aged calcite plate in (a) formation brine or (b) surfactant solution at 100 °C.

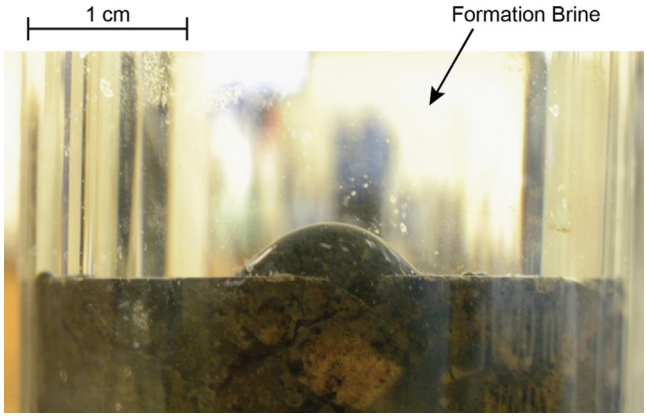

Fig. 5. The reservoir core immersed in formation brine after aging.

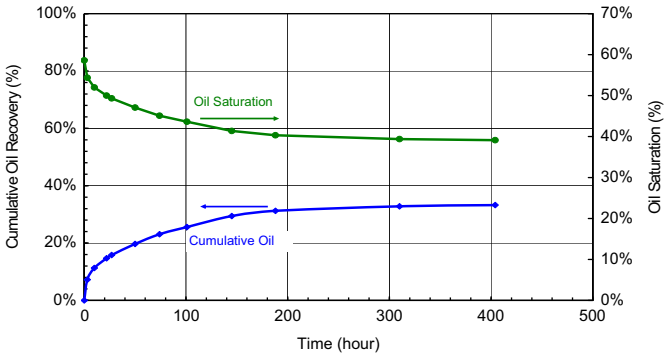

Fig. 6. Oil recovery and oil saturation from static imbibition experiment at 100 °C.

was produced when the core was immersed in the formation brine and no brine was imbibed. This indicates that the core was oil-wet. As shown in Fig. 5, oil droplets on top of the core tend to wet the solid, showing the contact angle is about 140°, which indicates that the oil-wetness of the core was restored after aging. Then the reservoir core was placed inside an imbibition cell surrounded by the surfactant solution containing 0.5 wt% C_{28}-25PO-25EO-carboxylate and 0.5 wt% C_{15-18}-IOS at the optimal salinity of 57,000 ppm. The surfactant formulation slowly imbibed into the core and expelled oil. The imbibition oil recovery reached 33.3% of the initial oil in 17 days, reducing the oil saturation to 0.39 as shown in Fig. 6. In this experiment, most of oil was observed to be produced from the top surface of the vertical core, which indicates that buoyancy is the most important driving force in this experiment.

4.3. CT scan analysis

A CT scan of the second core was conducted before and after the core was fractured. The images in Fig. 7 show that the reservoir core is extremely heterogeneous and vuggy before fractures were made. Some vugs are connected and some are isolated. Some parts of the core had higher vug density than other parts. The size of the vugs also varied over a wide range. The images in Fig. 8 show the core after it was fractured corresponding to the same cross-sections shown in Fig. 7. Some vugs are connected with fractures and some are not.

4.4. Coreflood

The brine permeability was 5.9×10^{-15} m^2 (6 md) before the core was fractured. After it was fractured, the permeability of the core was 1.9×10^{-12} m^2 (1970 md). The permeability contrast between fractures and matrix is similar to that of the fractured reservoir. Polymer was not used for mobility control due to the low matrix permeability. The surfactant solution was injected from the bottom at a low velocity of 7.1×10^{-7} m/s (0.2 ft/day) both to take advantage of buoyancy and to allow more time for imbibition and wettability alteration.

The water flood was conducted with formation brine at a frontal velocity of 4.2×10^{-5} m/s (12 ft/day). After the water flood, surfactant solution was injected to displace the oil at 100 °C. The formulation consisted of a mixture of 0.5 wt% C_{28}-25PO-25EO-carboxylate and 0.5 wt% C_{15-18}-IOS surfactants. A 0.25 pore volumes (PV) surfactant slug was injected followed by a brine drive. The initial (formation) brine had a salinity of about 117,000 ppm TDS with a divalent cation concentration of 4000 ppm. The salinity of the surfactant slug was 57,000 ppm TDS with a divalent cation concentration of 2300 ppm. The novel Guerbet alkoxy carboxylate and IOS surfactant mixture can tolerate such high temperature, high salinity and high hardness, and still produce ultra-low IFT and aqueous stability. After injection of the surfactant slug, about 1.46 PV brine was injected with a salinity of 10,000 ppm TDS. The chemical flood was stopped after about 1.71 PV of injection at an oil cut of about 5%.

The oil recovery data are shown in Fig. 9. The cumulative oil recovery was 65.9% of the remaining oil after the water flood, and the oil saturation decreased from 0.412 to 0.140. Compared with the static imbibition results, the coreflood showed higher oil recovery and the oil was produced at a faster rate. Because of the high permeability fractures, low injection rate and low viscosity of the injected surfactant solution, the pressure drop was nearly zero during the entire flood. The pressure drop data shown in Fig. 10 is very noisy due to the very low pressure drop and because of fluctuations caused by the back pressure regulator. The capillary pressure in the presence of surfactant was reduced to essentially zero, so capillary imbibition was negligible in the experiments. However, surfactant imbibition is driven by a transverse pressure gradient between the fractures and matrix that is induced by the buoyancy force related to the difference in density between the oil and water. Once the surfactant is in the matrix, it changes the wettability and reduces the IFT and both mechanisms increase the oil relative permeability. The oil can then flow upward due to buoyancy until it reaches a fracture and then it can flow in the fracture until it is produced. The trapping number is the sum of the capillary and Bond numbers for a vertical displacement (Pope et al., 2000). In this coreflood, the trapping number at this

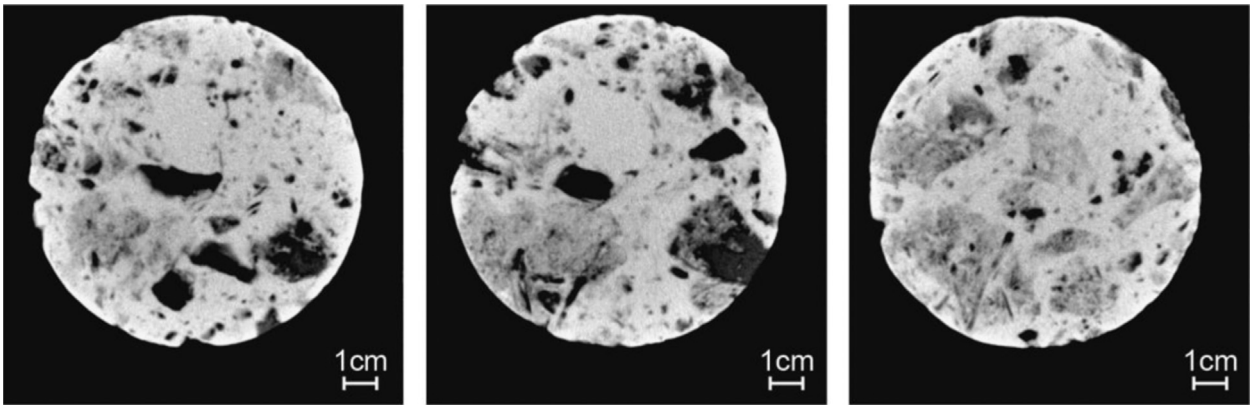

Fig. 7. CT images of the core before it was fractured.

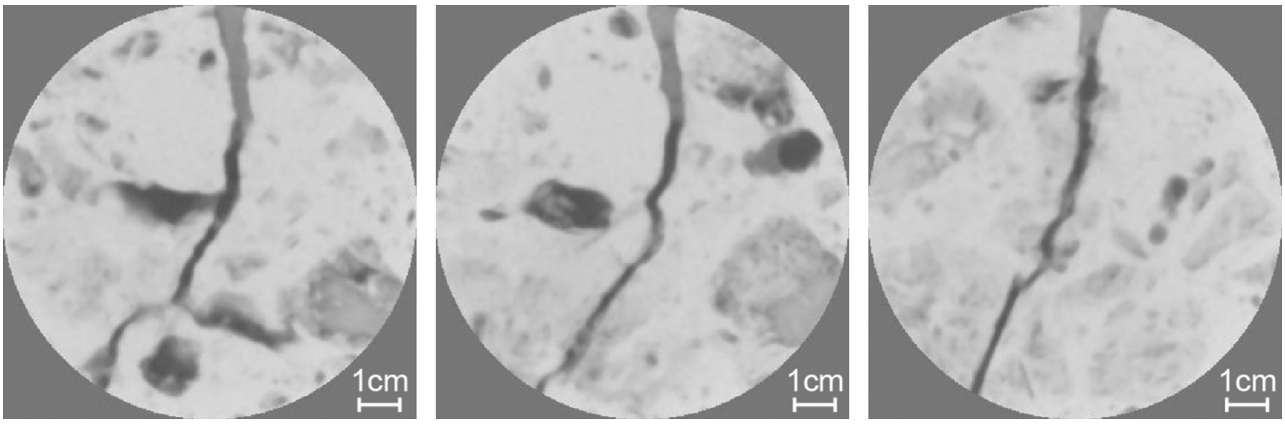

Fig. 8. CT images of the core after it was fractured.

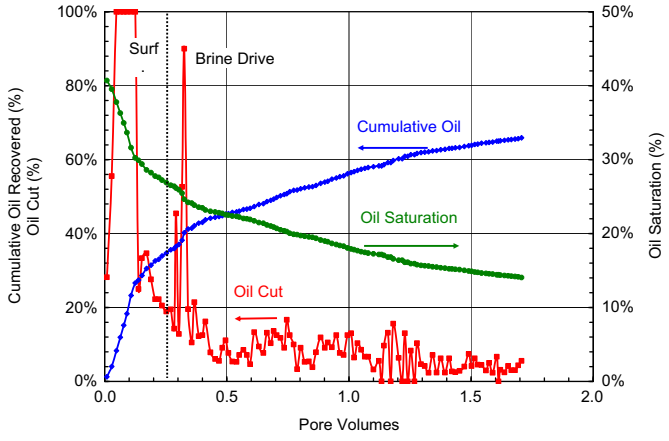

Fig. 9. Measured oil recovery, oil cut and oil saturation for coreflood.

ultra-low IFT is of the order of 0.001, which is consistent with a low chemical flood residual oil saturation. The trapping number is dominated by the buoyancy term in this experiment, or in other words it is approximately equal to the Bond number. Gravity is the most important force under these circumstances. Fig. 11 shows the produced surfactant concentration and salinity for this coreflood. No chromatographic separation between the two surfactants was observed. The total surfactant retention was 0.086 mg/g of rock with the individual contributions of 0.044 mg/g of C_{15-18}-IOS and 0.042 mg/g of C_{28}-25PO-25EO-carboxylate. The total surfactant retention value was low compared to other reported data (Wu et al., 2011). The initial effluent salinity was that of the initial brine, which decreased to the surfactant slug salinity, and then further decreased to the brine drive salinity. The surfactant was effective even though it mixed with the formation brine with a high hardness and salinity. The brine drive had a low enough salinity for the phase behavior of the surfactant to transition from Type II to Type III region, and eventually to Type I. The coreflood was successful in spite of the fact that (1) the core was extremely vuggy, fractured, and heterogeneous, (2) no mobility control (i.e. polymer) was used, and (3) only a small amount of surfactant was injected.

4.5. Simulation

UTCHEM was used to model the phase behavior, static imbibition and coreflood experiments. The phase behavior model in UTCHEM is based on Hand's rule (Hand, 1939) and uses the ternary diagram for representing different microemulsion phases and tie lines which are distributive curves. The tie lines which join the composition of the equilibrium phases are given as

$$\frac{C_{3l}}{C_{2l}} = E\left(\frac{C_{3l}}{C_{1l}}\right)^{F}, \quad for\ l = 1, 2,\ or\ 3 \tag{6}$$

where E and F are empirical parameters and ℓ refers to aqueous, oleic or microemulsion phase. For matching measured phase behavior data with UTCHEM model, parameters E and F were changed. The results are shown in Fig. 12. The current formulation in UTCHEM is a symmetrical binodal curve with the value of -1 for F and the value of E in Type I is 0.0028 and 0.00539 for Type II.

Fig. 13 shows a good match between the measured static imbibition data and the simulation. Figs. 14 and 15 compare experimental coreflood data and the simulation results using the

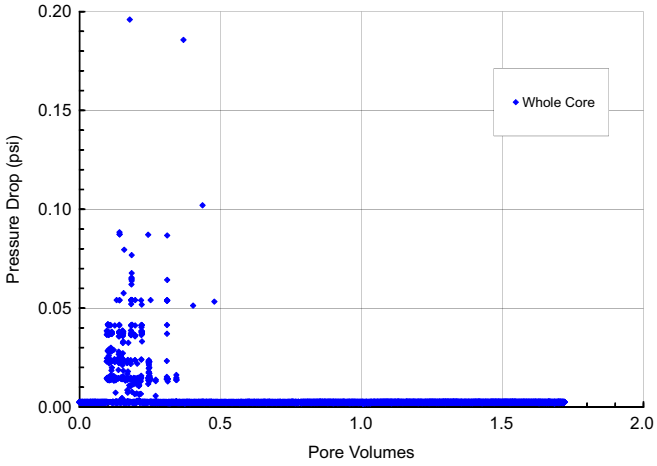

Fig. 10. Measured pressure drop during coreflood.

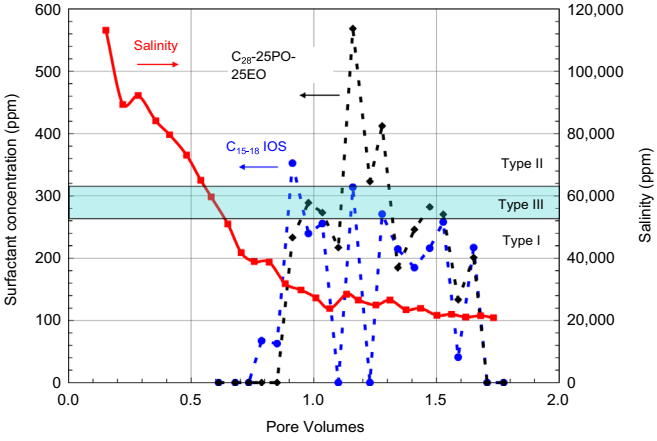

Fig. 11. Measured surfactant concentration and salinity of effluent from coreflood.

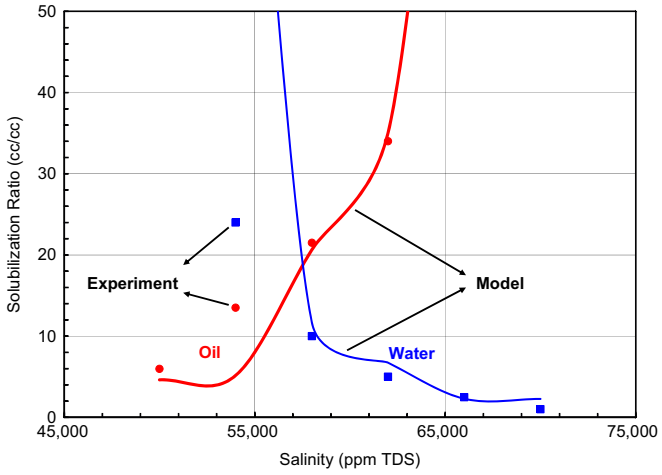

Fig. 12. Comparison of measured and modeled solubilization ratios at 100 °C.

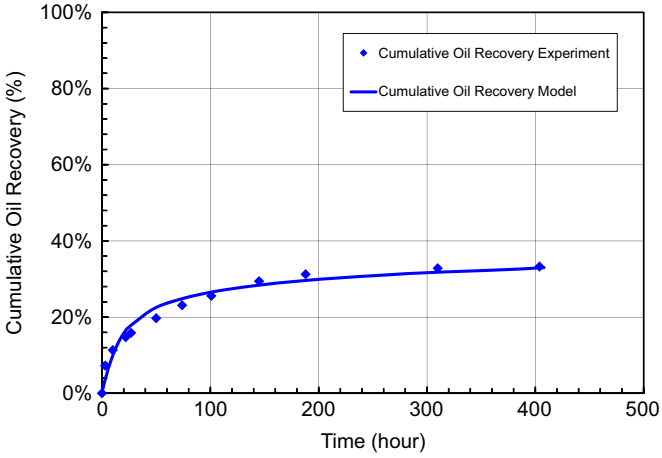

Fig. 13. Comparison of simulated and measured oil recovery for the static imbibition experiment.

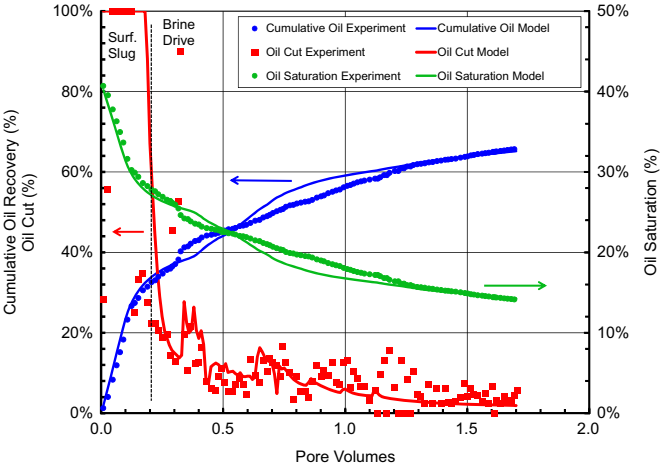

Fig. 14. Comparison of simulated and measured fractured coreflood results.

same model parameters. The relative permeability parameters were adjusted to match the oil recovery. Capillary pressure was neglected in these simulations. The relative permeability parameters are shown in Table 4. The oil relative permeability endpoint increased from 0.5 to 0.85 and water relative permeability endpoint decreased from 0.4 to 0.1, as shown in Fig. 16. The oil relative permeability endpoint increases during wettability alteration from mixed-wet to water-wet. However, for the water phase, the endpoint decreases during the transition from mixed-wet to water-wet.

Fig. 17 shows the sensitivity of the oil recovery to IFT reduction and wettability alteration mechanisms. Simulations with only one of these mechanisms gives lower oil recovery compared to including both mechanisms. The plot shows that the rate of oil recovery at early times for wettability alteration alone is lower than that due to IFT reduction alone.

The simulated oil saturation at the end of the flood and IFT at the end of surfactant injection are shown in Figs. 18 and 19. Fig. 18 is before surfactant breakthrough; the subsequent water injection pushes the surfactant slug through the core. These maps indicate that lower oil saturation correlates with lower IFT. The simulation was based on both IFT reduction and wettability alteration. The comparison of oil saturation distribution and the permeability distribution (in Fig. 1) illustrates that oil was mobilized even in low permeability grid blocks.

In the field, the surfactant solution would be injected in a horizontal well at the bottom of the fractured reservoir and the oil produced through another horizontal well placed at the top of the reservoir. The horizontal wells should be placed to connect to and flood the vertical fractures with the surfactant solution. Simulations should be used to optimize the field design after calibration with laboratory data such as those described in this paper. This paper reports three significant advances in surfactant flooding.

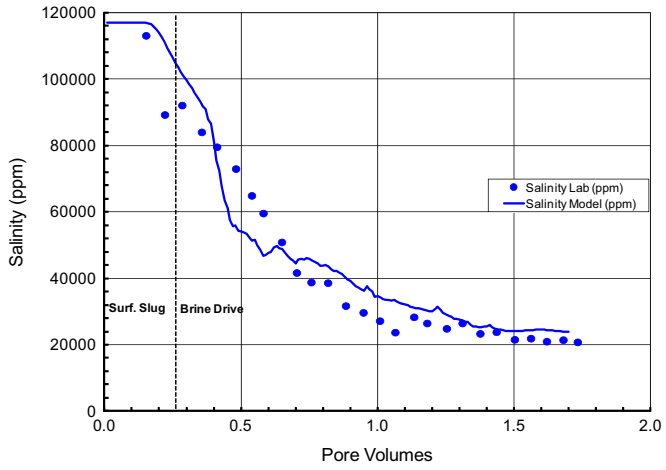

Fig. 15. Comparison of simulated and measured effluent salinity.

Table 4
Relative permeability parameters used in the simulation of coreflood.

Core data	Oil-wet		Water-wet	
	Oil	Water	Oil	Water
Residual saturation	0.18	0.50	0.05	0.50
Endpoint relative permeability	0.50	0.40	0.85	0.10
Relative permeability exponent	2.0	2.0	1.5	3.0
Scaling factor, ω_1	0.5			

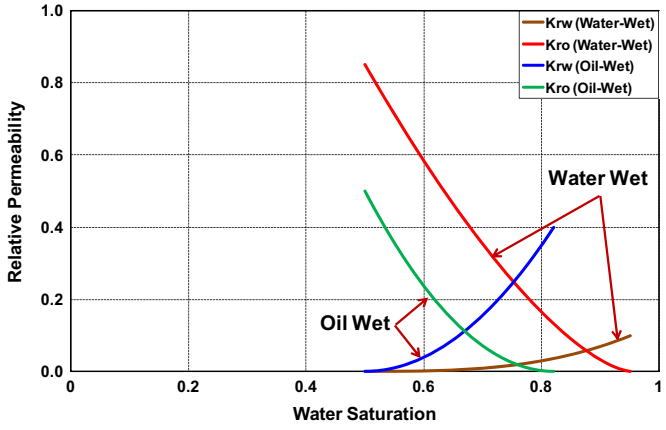

Fig. 16. Relative permeability curves at different wetting states.

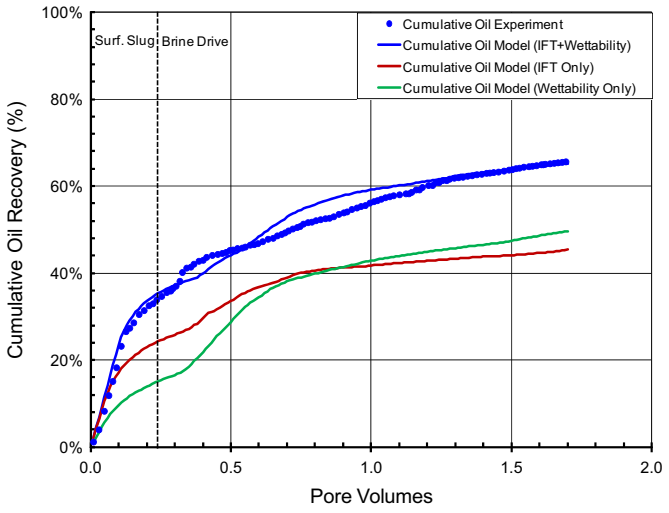

Fig. 17. Sensitivity simulations to IFT reduction and wettability alteration mechanisms.

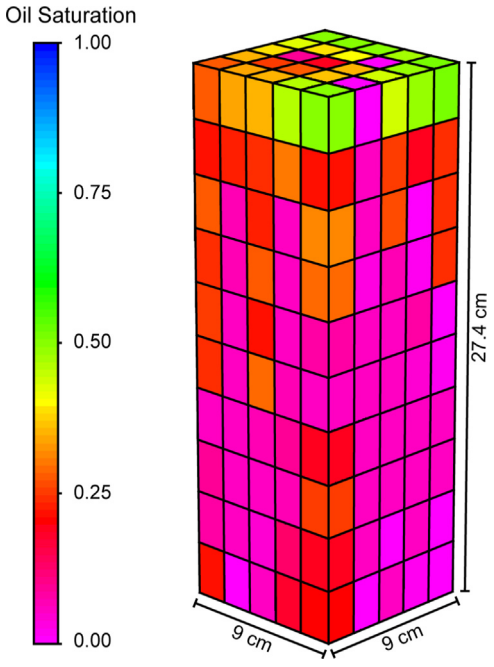

Fig. 18. Simulated oil saturation profile at 1.7 PV.

First, a surfactant system has been identified which are aqueous stable and achieves ultra-low interfacial tension at a high temperature and high salinity (with high hardness). Second, the surfactant system also alters the wettability of an initially oil-wet carbonate rock to a more water-wet state. Third, the surfactant flood enhances oil recovery in a fractured, vuggy core. The numerical modeling of the phase behavior and core flood helps develop relative permeability and wetting parameters that can be used in field simulations to estimate the efficacy of such surfactant floods in fractured reservoirs.

5. Conclusions

A surfactant formulation consisting of a novel large-hydrophobe Guerbet alkoxy carboxylate surfactant and an IOS co-surfactant was developed for a carbonate reservoir under high salinity and temperature. The surfactant both reduces the IFT to ultra-low values and alters the wettability of the rock toward more favorable water-wet conditions. Both static and dynamic core experiments were performed. In the dynamic coreflood experiment, the oil saturation was reduced to 0.14 using only a small amount of surfactant with no polymer. The surfactant retention was only 0.086 mg/g rock. The oil recovery is excellent taking into account that (1) the core was extremely vuggy and fractured, (2) no mobility control was used, and (3) only a small surfactant slug was injected. The oil recovery from the dynamic coreflood was higher than that for a similar static imbibition experiment. The UTCHEM simulator was used to match the coreflood data by using an extremely heterogeneous random permeability distribution to model the vuggy fractured core as opposed to attempting to model the fractures directly. It showed that both the mechanisms of IFT reduction and wettability alteration were dominant for oil recovery. Neither IFT reduction nor wettability alteration alone recovered oil as high as the combination of both

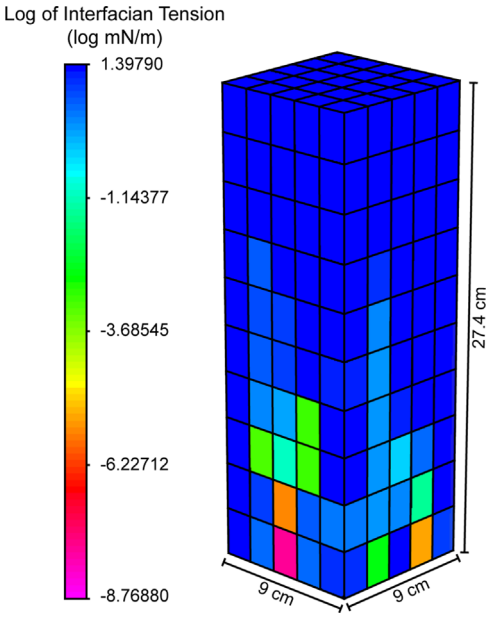

Fig. 19. Representation of IFT reduction at the end of surfactant flood.

mechanisms. Matching the experimental data is an important first step before using the simulator to predict field performance.

Acknowledgments

The authors would like to thank the industrial affiliates of the Chemical Enhanced Oil Recovery research project at The University of Texas at Austin for the financial support of this research. We would also like to acknowledge the resources, staff, and undergraduate research assistants of the Center for Petroleum and Geosystems Engineering at The University of Texas at Austin, and in particular we would like to thank Christopher Britton, Stephanie Adkins, Gayani P. Arachchilage, Sriram Solairaj, Mengyuan Chen, and Scott Hyde II for helping with the laboratory measurements, and Joanna Castillo for assistance with preparing the manuscript.

References

Abbasi-Asl, Y., Pope, G.A., Delshad, M., 24–28 April, 2010. Mechanistic modeling of chemical transport in naturally fractured oil reservoirs. In: Proceedings of SPE 129661 Presented at SPE IOR Symposium. Tulsa, OK.

Adibhatla, B., Mohanty, K.K., 22–26 April, 2006. Oil recovery from fractured carbonates by surfactant-aided gravity drainage: laboratory experiments and mechanistic simulations. In: Proceedings of SPE 99773 Presented at SPE IOR Symposium. Tulsa, OK.

Adkins, S., Arachchilage, G.P., Solairaj, S., Lu, J., Weerasooriya, U., Pope, G.A., 14–18 April, 2012. Development of thermally and chemically stable large-hydrophobe alkoxy carboxylate surfactants. In: Proceedings of SPE 154256 Presented at SPE IOR Symposium. Tulsa, OK.

Akbar, M., Chakravorty, S., Russell, S.D., Al Deeb, M.A., Efnik, R.S., Thower, R., Salman Mohamed S., 15–18 October, 2000. Unconventional approach to resolving primary and secondary porosity in gulf carbonates from conventional logs and borehole images. In: Proceedings of SPE 87297 Presented at the 9th Abu Dhabi International Petroleum Exhibition and Conference. Abu Dhabi, U.A.E.

Austad, T., Milter, J., 18–21 February, 1997. Spontaneous imbibition of water into low permeable chalk at different wettabilities using surfactants. In: Proceedings of SPE 37236 Presented at the SPE International Symposium on Oilfield Chemistry. Houston, Texas.

Austad, T., Matre, B., Milter, J., Saevareid, A., Oyno, L., 1998. Chemical flooding of oil reservoirs 8. Spontaneous oil expulsion from oil- and water-wet low permeable chalk material by imbibition of aqueous surfactant solutions. Colloids Surf. A: Phys. Eng. Asp. 137 (1–3), 117–129.

Bourbiaux, B., Fourno, A., Nguyen, Q.-L., Norrant, F., Robin, M., Rosenberg, E., Argillier, J.-F., 12–16 April, 2014. Experimental and numerical assessment of chemical EOR in oil-wet naturally-fractured reservoirs. In: Proceedings of SPE 169140 Presented at SPE IOR Symposium. Tulsa, OK.

Brühwiler, E., Wittmann, F.H., 1990. The wedge splitting test, a new method of performing stable fracture mechanics tests. Eng. Fract. Mech. 35 (1–3), 117–125.

Chen, P., Mohanty, K.K., 2013. Surfactant-mediated spontaneous imbibition in carbonate rocks at harsh reservoir conditions. SPE J. SPE 153960.

Chillenger, G.V., Yen, T.F., 1983. Some notes on wettability and relative permeability of carbonate rocks, II. Energy Sources 7 (1), 67–75.

Delshad, M., Najafabadi, N.F., Anderson, G.A., Pope, G.A., Sepehrnoori, K., 2009. Modeling wettability alteration in naturally fractured reservoirs. SPE Reserv. Eval. Eng. 12 (3), 361–370.

Flaaten, A.K., Nguyen, Q.P., Zhang, J., Mohammadi, H., Pope, G.A., 2008. ASP chemical flooding without the need of soft water. In: Proceedings of SPE 116754, Presented at SPE IOR Symposium. Tulsa, OK, April.

Goudarzi, A., Delshad,M., Mohanty,K.K, Sepehrnoori,K., 8–10 October, 2012. Impact of matrix block size on oil recovery response using surfactants in fractured carbonates. In: Proceedings of SPE 160219 Presented at SPE ATCE. San Antonio, TX.

Hand, D.B., 1939. Dineric distribution: I. The distribution of a consolute liquid between two immiscible liquids. J. Phys. Chem. 34, 1961–2000.

Hirasaki, G., Zhang, D.L., 2004. Surface chemistry of oil recovery from fractured, oil-wet, carbonate formations. SPE J. 9 (2), 151–162.

Huh, C., 1979. Interfacial tensions and solubilizing ability of a microemulsion phase that coexists with oil and brine. J. Colloid Interface Sci. 71, 408–426.

Iglauer, S., Wu, Y., Shuler, P.J., Tang, Y., Goddard, W.A., 2009. Alkyl polyglycoside surfactant-alcohol cosolvent formulations for improved oil recovery. Colloids Surf. A: Physicochem. Eng. Asp. 339, 48–59.

Iglauer, S., Wu, Y., Shuler, P.J., Tang, Y., Goddard, W.A., 2010. New surfactant classes for enhanced oil recovery and their tertiary oil recovery potential. J. Pet. Sci. Eng. 71 (1–2), 23–29.

Jang, S.H., Liyanage, P.J., Lu, J., Kim, D.H., Arachchilage, G.W.P.P., Britton, C., Weerasooriya, U., Pope, G.A., 12–16 April, 2014. Microemulsion phase behavior measurements using live oils at high temperature and pressure. In: Proceedings of SPE 169169 Presented at SPE IOR Symposium. Tulsa, OK.

Levitt, D.B., Jackson, A.C., Heinson, C., Britton, L.N., Malik, T., Dwarakanath, V., Pope, G.A., 2006. Identification and evaluation of high performance EOR surfactants. In: Proceedings of SPE 100089, Presented at SPE/DOE IOR Symposium. Tulsa, OK, April.

Lu, J., Britton, C., Solairaj, S., Liyanage, P.J., Kim, D.H., Adkins, S., Arachchilage, G.P., Weerasooriya, U., Pope, G.A., 2014a. Novel large-hydrophobe alkoxy carboxylate surfactants for enhanced oil recovery. SPE J. SPE 154256.

Lu, J., Liyanage, P.J., Solairaj, S., Adkins, S., Arachchilage, G.P., Kim, D.H., Britton, C., Weerasooriya, U., Pope, G.A., 2014b. New surfactant developments for chemical enhanced oil recovery. J. Pet. Sci. Eng. 120, 94–101.

Lu, J., Weerasooriya, U., Pope, G.A., 2014c. Investigation of gravity-stable surfactant floods. Fuel 124, 76–84.

Lu, J., 2014. Development of Novel Surfactants and Surfactant Methods for Chemical Enhanced Oil Recovery (Ph.D. dissertation). The University of Texas at Austin.

Morrow, N.R., Mason, G., 2001. Recovery of oil by spontaneous imbibition. Curr. Opin. Colloid Interfacial Sci. 6 (4), 321–337.

Pope, G.A., Wang, B., Tsuar, K., 1979. A sensitivity study of micellar/polymer flooding. SPE J., 357–368.

Pope, G.A., Wu, W., Narayanaswamy, G., Delshad, M., Sharma, M.M., Wang, P., 2000. Modeling relative permeability effects in gas-condensate reservoirs with a new trapping model. SPE J. 3 (2), 171–178.

Roehl, P.O., Choquette, P.W., 1985. Carbonate Petroleum Reservoirs. Springer-Verlag, New York.

Roshanfekr, M., Johns, R.T., Pope, G.A., Britton, L., Linnemeyer, H., Britton, C., Vyssotski, A., 2012. Simulation of the effect of pressure and solution gas on oil recovery from surfactant/polymer floods. SPE J. 17 (3), 705–716 (SPE 125095).

Sagi, A.R., Thomas, C.P., Bian, Y., Kwan, J.T., Salehi, M., Hirasaki, G.J., Puerto, M., Miller, C.A., 8–10 April 2013. Laboratory studies for surfactant flood in low-temperature, low-salinity fractured carbonate reservoir. In: Proceedings of SPE164062 Presented at International Symposium on Oilfield Chemistry. The Woodlands, Texas.

Seethepalli, A., Adibhatla, B., Mohanty, K.K., 2004. Physicochemical interactions during surfactant flooding of carbonate reservoirs. SPE J. 9 (4), 411–418.

Sharma, G., Mohanty, K.K., 2013. Wettability alteration in high-temperature and high-salinity carbonate reservoirs. SPE J. SPE 147306.

Solairaj, S., Britton, C., Lu, J., Kim, D.H., Weerasooriya, U., Pope, G.A., 14–18 April, 2012. New correlation to predict the optimum surfactant structure for EOR. In: Proceedings of SPE 154262 Presented at SPE IOR Symposium. Tulsa, OK.

Tong, Z.X., Morrow, N.R., Xie, X., 12–14 March, 2002. Spontaneous imbibition for mixed-wettability state in sand stones induced by adsorption from crude oil. In: Proceedings of 7th International Symposium on Reservoir Wettability. Tasmania, Australia.

Wang, L., Mohanty, K.K., 2014. Enhanced oil recovery in gasflooded carbonate reservoirs by wettability-altering surfactants. SPE J. SPE 166283.

Wu, Y., Iglauer, S., Shuler, P.J., Tang, Y., Goddard, W.A., 2011. Experimental analysis of surfactant retention on kaolinite clay. Tenside Surf. Deterg. 48 (5), 346–358.

Xie, X., Weiss, W.W., Tong, Z., Morrow, N.R., 2004. Improved oil recovery from carbonate reservoirs by chemical stimulation. SPE J. 10 (103), 276–285.

Zhang, D.L., Liu, S., Puerto, M., Miller, C.A., Hirasaki, G.J., 16–18 May, 2004. Wettability alteration and instantaneous imbibition in oil-wet carbonate formation. In: Proceedings of 8th International Symposium on Reservoir Wettability. Houston.

Zhang, J., Nguyen, Q.P., Flaaten, A.K., Pope, G.A., 19–23 April, 2008. Mechanisms of enhanced natural imbibition with novel chemicals. In: Proceedings of SPE 113453 Presented at SPE IOR Symposium. Tulsa, OK.
Zhao, P., Jackson, A.C., Britton, C., Kim, D.H., Britton, L.N., Levitt, D.B., Pope, G.A., 2008. Development of high-performance surfactants for difficult oils. In: Proceedings of SPE 113432, Presented at SPE/DOE IOR Symposium. Tulsa, OK, April.
Zhou, X., Morrow, N.R., Ma, S., 2000. Interrelationship of wettability, initial water saturation, aging time and oil recovery by spontaneous imbibition and waterflooding. SPE J. 5 (2), 199–207.